

## Effect of sodium benzoate on zinc electrodeposition in chloride solution

Yeqiang Mo · Qiming Huang · Weishan Li ·  
Shejun Hu · Meiling Huang · Youju Huang

Received: 17 December 2010 / Accepted: 25 March 2011 / Published online: 9 April 2011  
© Springer Science+Business Media B.V. 2011

**Abstract** The effect of sodium benzoate on the electrodeposition of zinc on carbon steel electrode from acidic chloride solution was studied by cyclic voltammetry (CV), differential capacitance (DC), chronoamperometry (CA), scanning electron microscopy (SEM), and X-ray diffraction (XRD). A dimensionless graph model was used to analyze the nucleation process of zinc. It is found that the sodium benzoate has a blocking effect on the zinc electrodeposition when its concentration is higher than 0.03 M but will accelerate the formation rate of zinc nuclei when its concentration is lower than 0.03 M. Benzoate can be adsorbed on the surface of the electrode, which reduces the interface tension of electrode/solution and favors the formation and growth of zinc nuclei when its concentration is lower than 0.03 M, but forms a separated layer and retards the formation and growth of zinc nuclei when its concentration is higher than 0.03 M.

**Keywords** Zinc · Electrodeposition · Chloride · Sodium benzoate

---

Y. Mo · Q. Huang · W. Li (✉) · S. Hu · M. Huang · Y. Huang  
School of Chemistry and Environment, South China Normal University, Guangzhou 510006, China  
e-mail: liwsh@scnu.edu.cn

Q. Huang · W. Li · S. Hu  
Key Laboratory of Electrochemical Technology on Energy Storage and Power Generation of Guangdong Higher Education Institutes, South China Normal University, Guangzhou 510006, China

Q. Huang · W. Li · S. Hu  
Engineering Research Center of Materials and Technology for Electrochemical Energy Storage (MOE), South China Normal University, Guangzhou 510006, China

### 1 Introduction

Electrodeposited zinc coating has found widespread application in the corrosion prevention of other metals such as carbon steel. Several plating electrolytes for zinc deposition have been used in industry, including cyanide, alkaline non-cyanide, and acid chloride solution [1]. Cyanide process is being prohibited due to its health and environmental pollution hazards as well as high effluent treatment costs [2]. Alkaline non-cyanide process, in spite of its non-toxicity, has several disadvantages such as low efficiency and strong corrosive attack [1, 3]. Comparatively, chloride process is of less cost and more environmental friendly and therefore is more attractive, especially for use in a high plating rate with maximum current efficiency [3, 4].

To obtain high quality plating, various organic additives are necessary for zinc plating in chloride solution [5]. The organic additives have been shown to affect the physical and mechanical properties of plating such as grain size, luster, uniformity, internal stress, and anti-corrosion [6, 7]. A number of organic additives have been reported for zinc plating in chloride solution and the effects of most organic additives on the zinc deposition have been well understood. Tripathy et al. [8] found that the lauryl sulphate increased current efficiency, reduced power consumption, and improved the surface morphology for the zinc electrodeposition in acidic solution. Gomes et al. [9] showed the effects of cetyl trimethyl ammonium bromide (CTAB), sodium dodecyl sulphate (SDS), and octylphenolpoly(ethylene glycoether)<sub>n</sub> ( $n = 10$ , Triton X-100) on the voltammetric behavior, structural, and morphological characteristics of the zinc deposition. Trejo et al. [10, 11] showed the effect of polyethoxylates and Mouanga et al. [12] showed the effect of coumarin on zinc electrodeposition in acidic

solution. It is found that most additives have a blocking effect on the zinc electrodeposition and improve the corrosion resistance of the deposited zinc. Moreover, there is a synergistic effect between additives such as benzalacetone and thiourea for the grain refinement of the deposited zinc [13].

Many proprietary combinations of the additives have been developed for zinc plating in chloride solution and sodium benzoate is one of the necessary components among these combinations [3, 14–16]. However, the effect of sodium benzoate on the zinc electrodeposition is less understood. In this study, the effect of sodium benzoate on the nucleation and growth of zinc were understood by cyclic voltammetry and chronoamperometry.

## 2 Experimental

The zinc plating bath was prepared by adding 0.37 M  $\text{ZnCl}_2$  and a certain concentration (0–0.06 M) of sodium benzoate in base solution of 0.57 M  $\text{H}_3\text{BO}_3$  + 2.7 M KCl (pH 5.0). All reagents were of analytical grade. In this article, the blank solution is 0.37 M  $\text{ZnCl}_2$  + 0.57 M  $\text{H}_3\text{BO}_3$  + 2.7 M KCl solution without additive.

The electrochemical experiments were carried out in a three electrode glass cell with a carbon steel disc (A3 steel, 0.5 cm in diameter) as working electrode, a platinum plate as counter electrode, and a commercial saturated calomel electrode (SCE) as reference electrode. The carbon steel disc was prepared by connecting a carbon steel rod electrically with copper wires, coating the rod with a masking paint and embedding it in epoxy resin, leaving the exposed working disc area. All the potentials in this article are reported with respect to SCE reference. Before each experiment, the working electrode was polished with silicon waterproof carbide paper (WESTEL), cleaned in deionized water ultrasonically for 3 min, and all the solutions were deaerated with  $\text{N}_2$  for 10 min.

All the electrochemical measurements were done at room temperature on PGSTAT-30 (Autolab, Eco Echemie B.V. Company). The cyclic voltammetry was carried out in the potentials between –0.4 and –1.6 V. The differential capacitance was measured at between –0.6 and 1.1 V under the 1000 Hz. The chronoamperometry was performed immediately after the working electrode was immersed in the solutions. The morphology of the electrodeposited zinc was observed using a scanning electron microscopy (JEOL, DSM-5400LV, JAPAN). The crystallinity of the electrodeposited zinc was characterized by X-ray diffraction on RIGAKU (D-MAX2200 VPC, JAPAN) with Cu-K $\alpha$  radiation from 30° to 90° at the rate of 0.1°/s.

## 3 Results and discussion

### 3.1 Voltammetric behavior of zinc in base solution

A typical cyclic voltammogram of A3 electrode in the base solution (0.57 M  $\text{H}_3\text{BO}_3$  + 2.7 M KCl) containing 0.37 M  $\text{ZnCl}_2$  is shown in Fig. 1. The voltammogram features the cathodic peak A at –1.18 V, corresponding to the zinc bulk deposition, and the wide anodic stripping peak B. The anodic stripping peak current is larger than the cathodic peak current, because zinc deposition takes place during backward and forward potential scanning between –1.0 and –1.6 V. The overpotential is necessary to initiate the formation of zinc nucleus on the A3 electrode, thus the current is hardly recorded at the potentials more positive than –1.0 V. As the potential becomes more negative, the current increases quickly, corresponding to the fast zinc deposition on the formed zinc nucleus. The involved reaction is [17]:



The zinc deposition process is inevitably accompanied by the hydrogen evolution reaction:



Upon the sweep reversal, there appear two crossovers between the cathodic and anodic currents at the potentials of –1.09 V ( $E_\eta$ ) and –1.06 V ( $E_c$ ), as shown in the inset of Fig. 1. The  $E_\eta$  is known as the nucleation overpotential [18] and the  $E_c$  is known as the crossover potential, which is equal to the reversible metal/ion potential [9]. The measured  $E_c$  is very close to the calculated thermodynamic potential (–1.07 V vs. SCE) [10]. The two current

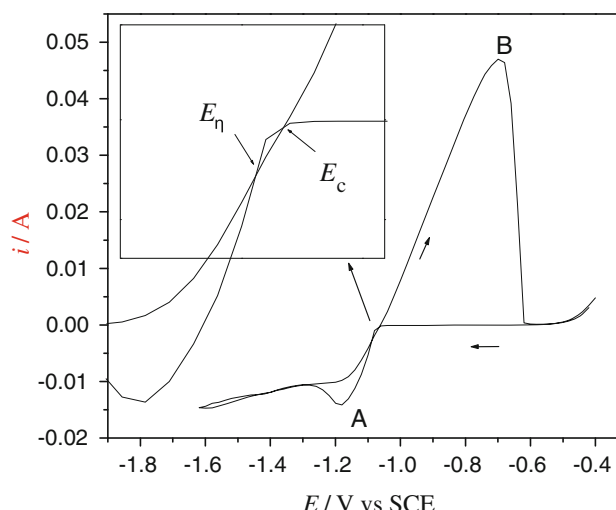


**Fig. 1** Cyclic voltammogram of A3 electrode in 0.37 M  $\text{ZnCl}_2$  + 0.57 M  $\text{H}_3\text{BO}_3$  + 2.7 M KCl solution. Scan rate: 20 mV s<sup>−1</sup>

crossovers are characteristic of nucleation processes. At the potentials more positive than the potential of peak B, the current approaches zero, indicating that the deposited zinc is removed from the A3 electrode.

Figure 2 presents the cyclic voltammogram of the A3 electrode in the base solution without  $Zn^{2+}$  ion. The potential scanning begins and ends at  $-0.4$  V. The reduction current can be observed at the potentials more negative than  $-1.1$  V and the oxidation current can be observed at the potentials more positive than  $-0.5$  V. The oxidation current can be ascribed to the oxidation of iron in A3 electrode, because the open circuit potential of A3 electrode in the base solution is  $-0.5$  V. The reduction current is mainly from hydrogen evolution and also includes the deposition of iron ions generated from the iron oxidation. The anodic peak C can be ascribed to the oxidation of the deposited iron. When adding sodium benzoate in the solution, the oxidation current of iron at the potentials more positive than  $-0.5$  V decreases significantly and the peak C in Fig. 2 disappears, as shown in Fig. 3. This suggests that the benzoate can be adsorbed on the surface of the A3 electrode and inhibits the iron dissolution.

### 3.2 Voltammetric behavior of zinc in the solutions containing sodium benzoate

Figure 4 presents the voltammograms of A3 electrode in the solutions containing different concentrations of sodium benzoate. Table 1 lists  $E_\eta$ ,  $E_c$ , and reduction peak potential obtained from Fig. 4. It can be seen from Table 1 that  $E_c$  is hardly affected by sodium benzoate while  $E_\eta$  (absolute value) decreases in the solution containing  $0.06$  M sodium benzoate, compared to that without sodium benzoate.  $E_c$  reflects the thermodynamic property of zinc and is related to the existing form for  $Zn^{2+}$  ion in the solution. The unchanged  $E_c$  suggests that sodium benzoate does not alter

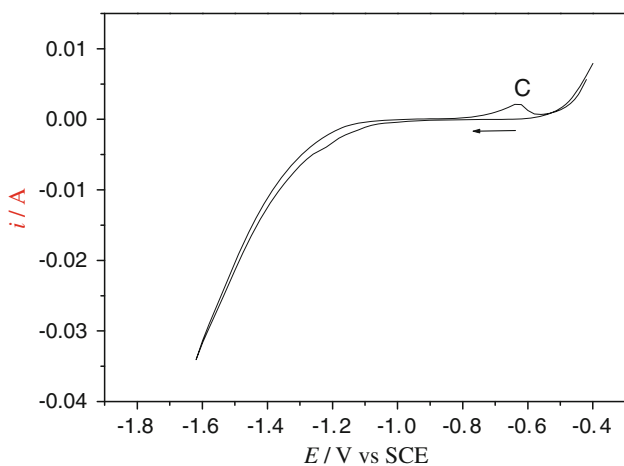


**Fig. 2** Cyclic voltammogram of A3 electrode in  $0.57$  M  $H_3BO_3$  +  $2.7$  M  $KCl$  solution. Scanning rate:  $20$  mV s $^{-1}$

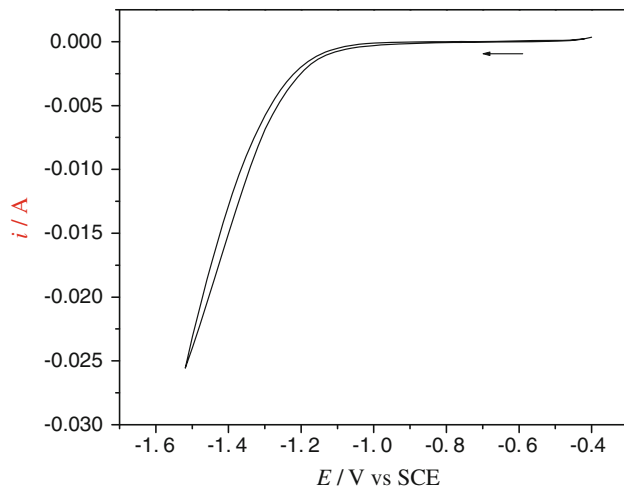


**Fig. 3** Cyclic voltammogram of A3 electrode in  $0.57$  M  $H_3BO_3$  +  $2.7$  M  $KCl$  +  $0.06$  M sodium benzoate solution. Scanning rate:  $20$  mV s $^{-1}$

the zinc deposition reaction (Eq. 1).  $E_\eta$  reflects the kinetics of zinc deposition. The changed  $E_\eta$  indicates that the kinetics of zinc deposition is affected by sodium benzoate. As shown in Table 1, the reduction peak potential becomes more negative and the reduction peak current becomes smaller in the solution with  $0.06$  M sodium benzoate than in the blank solution, confirming the blocking effect of sodium benzoate on the zinc electrodeposition. However, the reduction peak potential becomes more positive and the reduction peak current becomes larger in the solution with  $0.007$  M sodium benzoate than in the blank solution, suggesting that the zinc electrodeposition can be accelerated by sodium benzoate when its concentration is low.

It can be seen from Fig. 4 that the oxidation process of the deposited zinc in the solution containing sodium

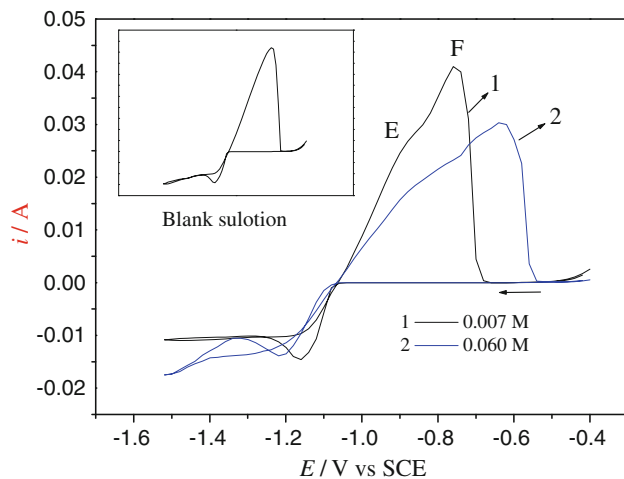


**Fig. 4** Cyclic voltammograms of A3 electrode in  $0.37$  M  $ZnCl_2$  +  $0.57$  M  $H_3BO_3$  +  $2.7$  M  $KCl$  + sodium benzoate solution. Scanning rate:  $20$  mV s $^{-1}$

**Table 1** Some parameters obtained from Fig. 4

Concentration of sodium benzoate (M)	$E_c$ (V)	$E_\eta$ (V)	Reduction peak potential (V)	Reduction peak current (A)
0	-1.06	-1.09	-1.18	-0.0140
0.007	-1.06	-1.09	-1.15	-0.0147
0.06	-1.07	-1.15	-1.21	-0.0137

benzoate is different from that in the blank solution. There are two peaks for the oxidation process of the deposited zinc, wide peak E and peak F, instead of the only one peak for that in the blank solution. This suggests that the crystal phase or the composition of the deposited zinc is affected by sodium benzoate, which can be ascribed to the combination of additives into zinc due to their adsorption [9, 10].

To confirm the adsorption of benzoate on electrode, differential capacitance curves were obtained, as shown in Fig. 5. It can be seen from Fig. 5 that the differential capacitance curves are significantly affected by sodium benzoate. The capacitance becomes smaller when sodium benzoate is used and decreases with increasing the concentration of sodium benzoate, indicating that benzoate can be adsorbed on the surface of the electrode. The adsorption of benzoate on the electrode must change the interface properties of electrode/solution and therefore affects the zinc deposition process and the phase structure or composition of the deposited.

### 3.3 Chronoamperometric response

Figure 6 presents the chronoamperometric responses of A3 electrode in 0.37 M  $\text{ZnCl}_2$  + 0.57 M  $\text{H}_3\text{BO}_3$  + 2.7 M

KCl solution. It can be seen from Fig. 6 that the chronoamperometric responses in all the cases (under different potentials or in the solutions containing different sodium benzoate concentrations) are characteristic of a nucleation process [10, 19–24]. The currents rise at the beginning, reach a maximum value (denoted as  $i_m$ ) at certain time (denoted as  $t_m$ ) and then decrease. The rise in current reflects the formation and growth of zinc nuclei on A3 electrode and the decrease of the current reflects the diffusion-controlled process for zinc deposition. It can be seen from Fig. 6a that  $i_m$  increases but  $t_m$  decreases as the polarized potential becomes more negative. This phenomenon can be ascribed to the increase in formation and growth rate of zinc nuclei due to larger polarized potential [10, 25].

It can be noted from Fig. 6b that  $i_m$  is larger but  $t_m$  is shorter for the formation and growth of zinc nuclei in the solution containing 0.007 and 0.013 M sodium benzoate than in the blank solution, while  $i_m$  decreases and  $t_m$  increases as the concentration of sodium benzoate increases further. This suggests that the formation and growth rate of zinc nuclei is accelerated in the solution containing a low concentration of benzoate and is retarded in the solution containing a high concentration of benzoate. This result is in agreement with that obtained from cyclic voltammograms (Fig. 4 and Table 1). The retardance is prevalent but the acceleration is not observed for the effect of other additives on the metal electrodeposition [26].

The effect of sodium benzoate on the formation and growth of zinc nuclei can be explained as follows. Based on the analysis of differential capacitance curves (Fig. 5), the benzoate can be adsorbed on the electrode. The adsorption of benzoate reduces the interface tension of electrode/solution and thus favors the formation and growth of zinc nuclei. On the other hand, the adsorbed benzoate separates the electrode from the solution, which retards the formation and growth of zinc nuclei. In the solution containing a low concentration of benzoate, the reduction of the interface tension dominates, resulting in the accelerated formation and growth of zinc nuclei. In the solution containing a high concentration of benzoate, the separation dominates resulting in the retarded formation and growth of zinc nuclei.

There are two models for the crystal nucleation and growth during metal electrodeposition: instantaneous and progressive [10, 25, 27, 28]. In the instantaneous nucleation

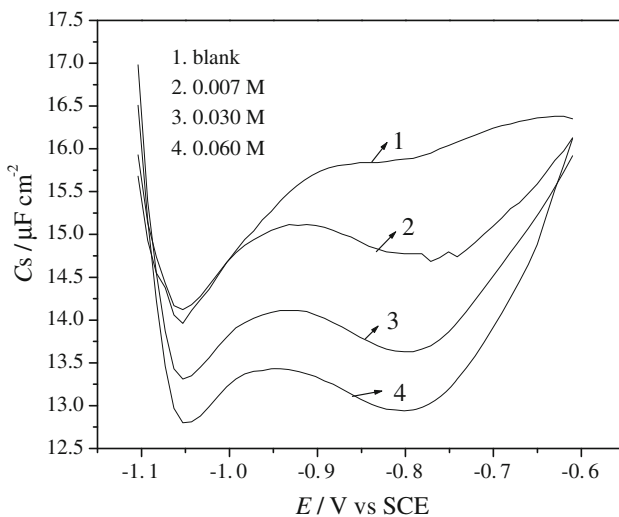


**Fig. 5** Differential capacitance versus potential curves for A3 electrode in 0.37 M  $\text{ZnCl}_2$  + 0.57 M  $\text{H}_3\text{BO}_3$  + 2.7 M KCl + sodium benzoate solution

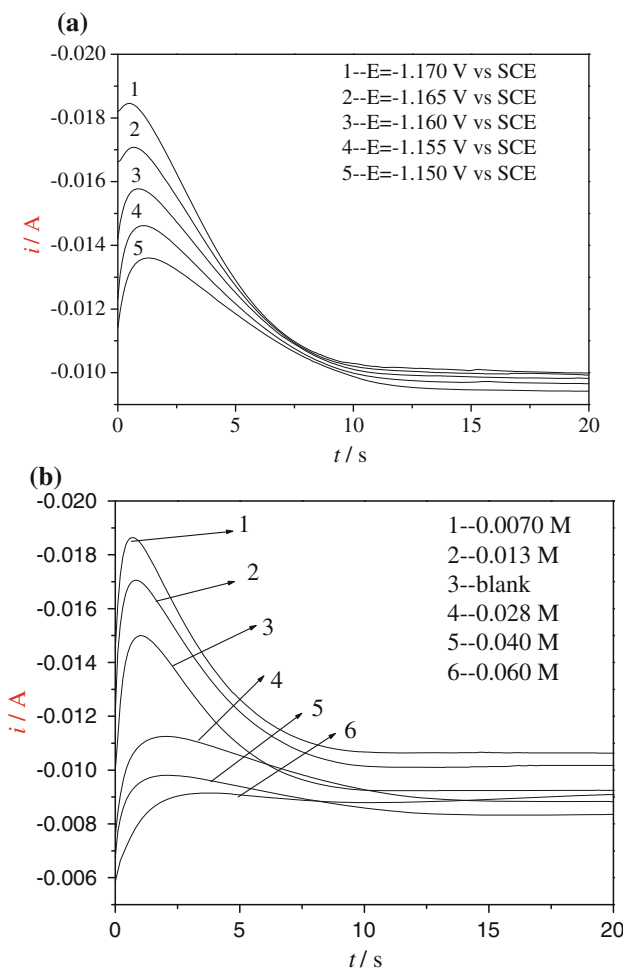


**Fig. 6** Chronoamperometric curves of A3 electrode in 0.37 M  $\text{ZnCl}_2$  + 0.57 M  $\text{H}_3\text{BO}_3$  + 2.7 M KCl + sodium benzoate solution, **a** the effect of potential, 0.04 M sodium benzoate; **b** the effect of sodium benzoate concentration at  $-1.14$  V versus SCE

process, the number of nuclei is large and all the active sites of electrode are covered instantaneously by nuclei, the relation of current ( $i$ ) with time ( $t$ ) follows:

$$\left(\frac{i}{i_m}\right)^2 = 1.9542 \left(\frac{t}{t_m}\right)^{-1} \left\{ 1 - \exp \left[ -1.2564 \left(\frac{t}{t_m}\right) \right] \right\}^2 \quad (3)$$

In the progressive process, the number of nuclei is assumed to be a time dependent function, the relation of current with time follows:

$$\left(\frac{i}{i_m}\right)^2 = 1.2254 \left(\frac{t}{t_m}\right)^{-1} \left\{ 1 - \exp \left[ -2.3367 \left(\frac{t}{t_m}\right)^2 \right] \right\}^2 \quad (4)$$

Figure 7 presents experimental relation of current with time in dimensionless for the zinc deposition in three kinds of solutions (free, low, and high concentrations of sodium

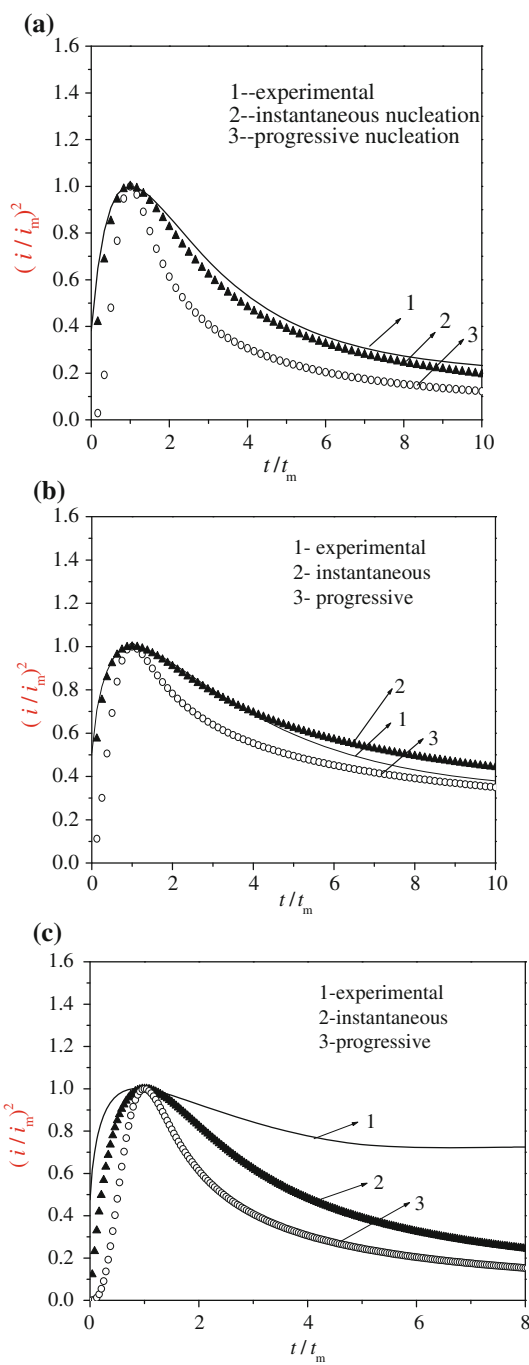


**Fig. 7** Comparison between the theoretical dimensionless graphs for instantaneous and progressive nucleation and the experimental nucleation process for zinc deposition from 0.37 M  $\text{ZnCl}_2$  + 0.57 M  $\text{H}_3\text{BO}_3$  + 2.7 M KCl solutions containing 0 M (a); 0.013 M (b); 0.040 M (c)

benzoate) along with the fitting results based on Eqs. 3 and 4. In the solution without sodium benzoate (Fig. 7a), the experimental results can be well fitted by the instantaneous nucleation model (Eq. 3), indicating that the formation and growth of zinc nuclei in the solution without sodium benzoate follows an instantaneous nucleation process.

**Fig. 8** SEM images of electrodeposited zinc obtained in 0.37 M  $\text{ZnCl}_2$  + 0.57 M  $\text{H}_3\text{BO}_3$  + 2.7 M KCl solutions containing 0 M (a); 0.007 M (b); 0.03 M (c); 0.04 M (d) at  $-1.16$  V versus SCE for 40 s

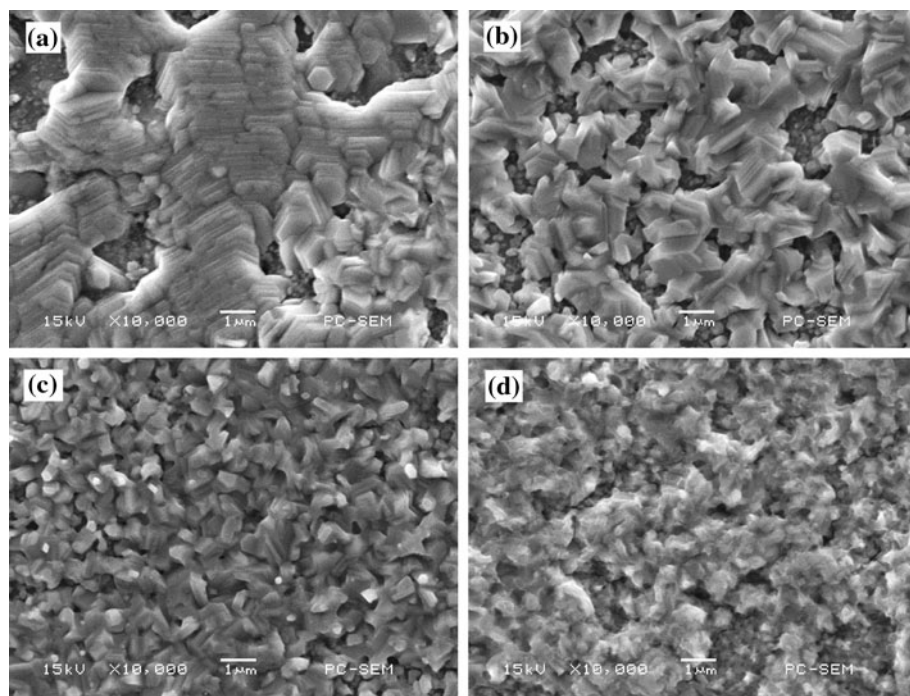
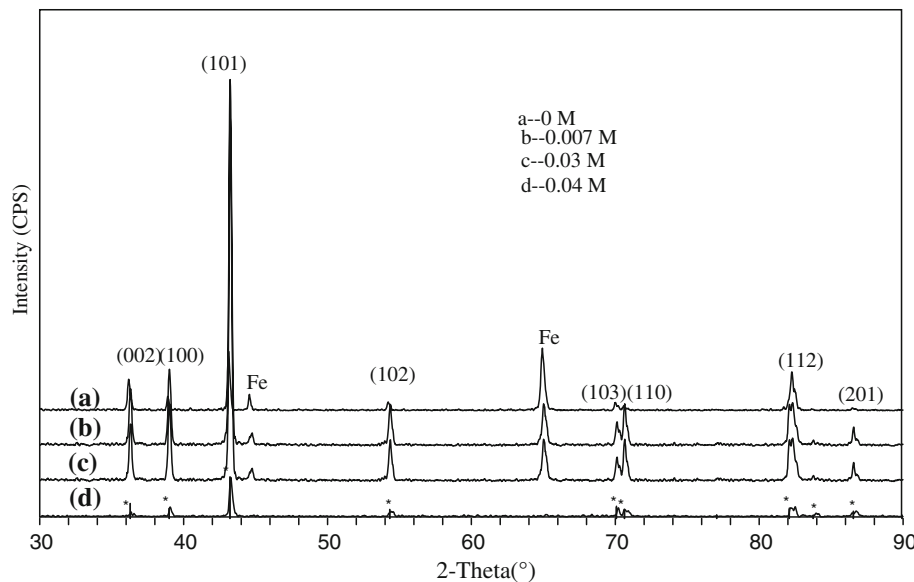


**Fig. 9** X-ray patterns of electrodeposited zinc obtained in 0.37 M  $\text{ZnCl}_2$  + 0.57 M  $\text{H}_3\text{BO}_3$  + 2.7 M KCl solutions containing 0 M (a); 0.007 M (b); 0.03 M (c); 0.04 M (d) at  $-1.16$  V versus SCE for 40 s



However, different results are obtained in the solutions containing sodium benzoate, as shown in Fig. 7b, c.

It can be seen from Fig. 7b that the relation of current time can be well fitted by the instantaneous nucleation model (Eq. 3) at the initial stage ( $t/t_m < 4$ ) for the zinc electrodeposition and approaches to the progressive model (Eq. 4) at the latter stage. This suggests that the zinc electrodeposition process can be affected by the low concentration of benzoate but the nucleation mechanism is the same as that in the blank solution. Therefore, the nucleation

mechanism for the zinc electrodeposition is not affected by the low concentration of benzoate. In the solution containing the high concentration of benzoate, the relation of current with time cannot be well fitted by the instantaneous nucleation model (Eq. 3) or by the progressive model (Eq. 4). This suggests that not only the nucleation of zinc but also the progression of the deposited zinc are affected by the high concentration of benzoate and confirms the explanation that a separated layer of adsorbed benzoate retards the formation and growth of zinc nuclei.

**Table 2** The full width at half maximum (FWHM) obtained from Fig. 9

Concentration (M)	(002)	(100)	(101)	(102)
0	0.174	0.071	0.157	0.094
0.007	0.183	0.182	0.186	0.198
0.03	0.190	0.189	0.168	0.196
0.04	0.206	0.235	0.247	0.342

### 3.4 Crystal structure of electrodeposited zinc

It is well known that the crystal structure of an electrodeposited metal is usually affected by the application of an organic additive [5, 10, 29]. To understand the effect of sodium benzoate on the crystal structure of the electrodeposited zinc, SEM and XRD characterization were performed for the samples deposited on a carbon steel substrate in the solutions containing different concentrations of benzoate at  $-1.16$  V versus SCE for 40 s.

Figure 8 presents the SEM images of the samples. It can be seen from Fig. 8a that the zinc deposited in the solution without sodium benzoate is composed of big hexagonal crystals. When adding benzoate in the solution, the crystal size of the deposited zinc becomes smaller, as shown by Fig. 8b or c. In the solution containing 0.04 M benzoate, the deposited zinc becomes smallest, as shown in Fig. 8d.

Figure 9 presents the XRD patterns of the samples. Table 2 lists the full width at half maximum (FWHM) of orientation from Fig. 9. All the samples have the diffraction of iron, which can be ascribed to the substrate. It can be seen from Fig. 9a that the zinc deposited in the solution without benzoate have the diffractions at the crystal planes of (002), (100), (101), and (102), which are characteristic of hexagonal crystal (JCPDS card No. 65-3358) and confirms the observation by SEM. When adding a low concentration (0.007 or 0.03 M) of benzoate, the diffraction peak intensity of the deposited zinc increases at (002), (100), (101), and (102) orientations, as shown by Fig. 9b or c. This indicates that benzoate affects the preferred orientation of zinc deposition. In the solution containing 0.04 M benzoate, the diffraction peaks at (002), (100), and (112) almost disappear, confirming that the deposited zinc tend to be amorphous. Therefore, the morphology and crystal structure of the electrodeposited zinc can be affected by sodium benzoate.

## 4 Conclusions

Like other additives, sodium benzoate affects the zinc electrodeposition process in chloride solution and the morphology of the electrodeposited zinc through its adsorption

on electrode. However, different from the effects of other additives, when sodium benzoate's concentration is lower than 0.03 M, it accelerates the formation rate of zinc nuclei. This acceleration can be ascribed to the reduction of interface tension between electrode/solution. When its concentration is higher than 0.03 M, the sodium benzoate has a blocking effect on the zinc electrodeposition.

**Acknowledgments** This study was supported by Specialized Research Fund for the Doctoral Program of Higher Education (Grant No. 200805740004) and Natural Science Foundation of Guangdong Province (Grant No. 10351063101000001).

## References

- Shanmugasigamani S, Pushpavanam M (2006) J Appl Electrochem 36:315
- Sekar R, Jayakrishnan S (2006) J Appl Electrochem 36:591
- Schlesinger M, Paunovic M (2000) Modern electroplating, 4th edn. John Wiley & Sons Inc, New York
- Pereira MS, Barbosa LL, Souza CAC et al (2006) J Appl Electrochem 36:727
- Lee JY, Kim JW, Lee MK (2004) J Electrochem Soc 151:C25
- Méndez PF, López JR, Meas Y (2005) Electrochim Acta 50:2815
- De Oliveira EM, Carlos IA (2008) J Appl Electrochem 38:1203
- Tripathy BC, Das SC, Heftet GT et al (1997) J Appl Electrochem 27:673
- Gomes A, Da Silva Pereira MI (2006) Electrochim Acta 52:863
- Trejo G, Ruiz H, OrtegaBorges R et al (2001) J Appl Electrochem 31:685
- Trejo G, Ortega R, Meas Y et al (1998) J Electrochem Soc 145:4090
- Mouanga M, Ricq L, Douglade G et al (2006) Surf Coat Tech 201:762
- Li MC, Jing LL, Zhang WQ et al (2007) J Solid State Electrochem 11:549
- Shpan'ko SP, Grigor'ev VP, Dymnikova OV et al (2004) Prot Met 40:316
- Van den Bos C, Schnitger HC, Zhang X et al (2006) Corros Sci 48:1483
- Díaz-arista P, Meas Y, Ortega R et al (2005) J Appl Electrochem 35:217
- Ballesteros JC, Díaz-Arista P, Meas Y et al (2007) Electrochim Acta 52:3686
- Fletcher S (1983) Electrochim Acta 28:917
- Torrent-Burgués J, Guaua EJ (2007) J Appl Electrochem 37:643
- Gladysz O, Los P (2008) Electrochim Acta 54:801
- Hovestad A, Heesen RJCHL, Janssen LJJ (1999) J Appl Electrochem 29:331
- Garfias-García E, Romero-Romo M, Ramírez-Silva MT et al (2008) J Electroanal Chem 613:67
- Abyaneh MY, Fleischmann M, Del Giudice E et al (2009) Electrochim Acta 54:879
- Bozzini B, D'Urzo L, Mele C (2007) Electrochim Acta 52:4767
- Ferapontova EE, Terry JG, Walton AJ et al (2007) Electrochim Commun 9:303
- Gu M, Yang FZ, Huang L et al (2002) Acta Chim Sin 60:1946
- Scharifker B, Hills G (1983) Electrochim Acta 28:879
- Vasilakopoulos D, Bouroushian M, Spyrellis N (2009) Electrochim Acta 54:2509
- Baik DS, Fray DJ (2001) J Appl Electrochem 31:1141